Available online at www.sciencedirect.com
SCIENCE DIRECT®
Journal of Power Sources 132 (2004) 181–186
JOURNAL OF POWER SOURCES
www.elsevier.com/locate/jpowsour

All solid-state rechargeable lithium cells based on nano-sulfur composite cathodes

Xianguo Yu [a,*], Jingying Xie [a], Jun Yang [b], Ke Wang [a]

[a] *Energy Science and Technology Laboratory, Shanghai Institute of Microsystem and Information Technology, Chinese Academy of Sciences, Shanghai 200050, China*

[b] *Department of Chemical Engineering, Shanghai Jiao Tong University, Shanghai 200240, China*

Received 8 October 2003; received in revised form 14 January 2004; accepted 16 January 2004

Abstract

Charge–discharge properties of a new type of all solid-state lithium cell are presented, which comprises a conductive nano-sulfur composite (NSC) cathode, composite polymer electrolyte based on poly(ethylene oxide), $LiN(CF_3SO_2)_2$ and nano-sized TiO_2 filler and lithium anode. The cell exhibits high discharge capacity up to 600 mAh g^{-1} (referred to the NSC active material, EO/Li = 8 for polymer electrolyte) at the second cycle and about 385 mAh g^{-1} at the 40th cycle at operation temperature of 70 °C. The electrochemical characteristics of the nano-composite polymer electrolyte, related to the performance of cells, are also examined in detail.
© 2004 Elsevier B.V. All rights reserved.

Keywords: Polymer electrolyte; Rechargeable lithium cells; Sulfur-containing composite; Poly(ethylene oxide); Ceramic filler

1. Introduction

All solid-state lithium/polymer battery (LPB), based on metallic lithium anode and dry polymer electrolyte, has been regarded as candidate of next generation of high performance lithium batteries due to the high safety and reliability, large energy density, and flexible shape fabrication. Great attention has been paid to two important research directions in the field of LPBs in recent years. One is the enhancement of the ionic conductivity and stability of dry polymer electrolytes. Another involves the development of suitable cathode active materials matching the polymer electrolytes in lithium batteries.

Among the polymer electrolyte materials reported, poly(ethylene oxide)–lithium salt (PEO–LiX) complexes have been investigated most widely because of the more stability and higher ionic conductivity than those containing any other group of solvating polymers without the addition of organic solvents [1–4]. However, the ionic conductivity of PEO–LiX electrolyte remains very low ($\leq 10^{-6}$ S cm^{-1}) at room temperature due to the crystalline nature of PEO, and therefore, only at high temperatures can reach practically useful values ($\geq 10^{-4}$ S cm^{-1}). Various methods have been introduced to enhance the ionic conductivity [5–9], and one of the successful approaches is to add ceramic nanoparticles such as TiO_2, $LiAlO_2$ or SiO_2 to PEO–LiX or PEO-like polymers [10–12]. The addition of nano-sized ceramic powders can not only enhance the ionic conductivity, but also improve the mechanical property and interfacial compatibility with metallic lithium [13]. On the other hand, the electrochemical stability against a high voltage is also very important for cycling performance and safety, because there is a tendency towards decomposition of PEO chains kinetically when operating at relatively high potentials. The breakdown voltage of PEO-based electrolyte membranes evaluated by linear sweep voltammetry (LSV) or cyclic voltammetry (CV) on a smooth stainless steel blocking electrode is usually above 4 V versus Li/Li^+ [14–16]. However, in a real battery system, the polymer electrolyte contacts with a composite cathode containing active material and conductive agent, e.g., carbon black, acetylene black, etc. The catalysis of carbon with large surface facilitates the decomposition of polymer at 3.8 V versus Li/Li^+ or even a little lower voltage [17]. Obviously, the so-called 4 V cathode materials such as $LiCoO_2$, $LiNiO_2$ and $LiMn_2O_4$, appear not to be the best selection for such LPB systems with PEO-like electrolytes. So, it is necessary to adopt cathode materials with less-positive intercalation potentials and a large capacity. In spite of a typical discharge voltage below 3.5 V versus Li/Li^+, vanadium and manganese oxides have much lower Li-insertion capacity [18–20] than elemental sulfur whose theoretical specific capacity reaches

* Corresponding author. Tel.: +86-21-62131647; fax: +86-21-32200534.
E-mail address: yuxg@mail.sim.ac.cn (X. Yu).

0378-7753/$ – see front matter © 2004 Elsevier B.V. All rights reserved.
doi:10.1016/j.jpowsour.2004.01.034

1672 mAh g^{-1}. Unfortunately, elemental sulfur is difficult to be utilized as cathode active material because the batteries with sulfur electrode suffers from rapid capacity fading due to the fact that polysulfides, which are formed during the discharge process, dissolves in the liquid electrolytes [21–24]. The electrochemical properties of lithium/sulfur batteries with gel-type polymer electrolyte have also been investigated, but the specific capacity based on active material of sulfur or sulfide is far below 200 mAh g^{-1} even just only running 10 cycles [25].

Recently, a novel conductive nano-sulfur composite (NSC) cathode material was synthesized in our research group. In this composite, sulfur nanoparticles are embedded in the heterocyclic structure of the dehydrogenated product of polyacrylonitrile and sulfur contacts with conductive dehydrogenated product in the molecular level. The NSC exhibits specific capacity of more than 600 mAh g^{-1} and capacity fade rate of about 26% after 50 cycles in gel-type polymer electrolyte cells, improving the charge–discharge performance of elemental sulfur to some extent [26]. However, as long as the existence of liquid solvents in the electrolytes, degradation and instability of the lithium anode are inevitable. In addition, a small amount of the discharge products of NSC may also dissolve in the liquid solvent, leading to the capacity fade. Dry polymer electrolytes, such as PEO–LiX complex, may be able to reduce the reactivity with lithium and restrain the dissolution of the discharge products into the electrolyte.

In the present paper, all solid-state cells using NSC cathode active material and nanocomposite PEO polymer electrolytes (CPE) containing nano-sized ceramic TiO_2 particles are prepared and the electrochemical charge–discharge behaviors are investigated.

2. Experimental

2.1. Preparation of nanocomposite polymer electrolyte

The nanocomposite polymer electrolytes were prepared by combining polyethylene oxide (Aldrich chemical Co., $M_n = 4 \times 10^6$), with lithium salt $LiN(CF_3SO_2)_2$ (LiTFSI, from Fluka) and ceramic nano-TiO_2 filler (Zhou shan nanotech. Co., $\phi 25 \pm 5$ nm). Unless stated otherwise, molar ratio of oxygen/lithium (EO/Li) was fixed to 20 and the amount of the nano-TiO_2 to 8% of the total PEO_{20}LiTFSI weight. The preparation of the electrolytes involved first the dispersion of the selected nano-TiO_2 and dissolution of the LiTFSI in acetonitrile solvent, followed by the addition of 20 wt.% of the whole PEO under ultrasonic stirring for 30 min, and finally the addition of remnant PEO component. The obtained slurry was magnetically stirred for 24 h and then cast into a Teflon disc plate (ϕ9 cm). The solvent in the slurry was allowed to evaporate slowly and the mechanically sustainable membranes (average thickness ca. 150–180 μm) were obtained after drying under vacuum at 80 °C for 24 h.

2.2. Preparation of composite cathode

The new type of active material, NSC, was synthesized by heating a mixture of polyacrylonitrile (PAN) and elemental sulfur as described previously [26]. The composite cathode film mainly comprised active material of NSC, conductive agent of acetylene black (AB) and electrolyte component PEO_{40}LiTFSI. In order to improve the ionic conductivity and wetting properties, the proper amount of low-molecular-weight poly(ethylene glycol) (PEG, Mw = 1000) was also added into the cathode. For facilitating to form the mechanically sustainable cathode films, the EO/Li molar ratio is kept 40 (counted as the PEO) in the electrolyte component of composite cathode, in which the PEO also acts as binder. The preparation of composite cathode was similar to that of the polymer electrolytes and its average thickness was 70–90 μm. A typical composition of the cathode was—40 wt.% NSC, 12 wt.% AB, 48 wt.% PEO_{40}(PEG) LiTFSI.

2.3. Electrochemical measurements

The ionic conductivity of the polymer electrolytes and the Li/electrolyte interface stability were studied by ac impedance spectroscopy, using an EG&PAR potentiostat coupled with a Solartron Model 1260 frequency response analyzer. Stainless steel blocking electrode cells were used for conductivity measurements, and symmetrical non-blocking lithium electrode cells were taken to examine interface compatibility by monitoring the resistance change over time at 70 °C. The impedance spectrum was normally recorded from 100 kHz to 0.1 Hz, and the ac amplitude was 5 mV. The ionic conductivity (σ) was calculated from the electrolyte resistance (R_b) obtained from the intercept of the real axis of an impedance spectrum, the film thickness (l), and the electrode area (A) using the equation $\sigma = l/AR_b$. The Solartron potentiostat Model S1 1287 electrochemical interface was also used for cyclic voltammetry of the cells with lithium both as counter and reference electrodes.

2.4. Cell assembling and testing

CR2025-type coin cells were fabricated by sandwiching the CPE between the composite cathode and lithium metal in a glove box. Before the cycling test, they were preheated for 2 h at 80 °C in order to insure a good interface contact between the electrolyte and electrodes. The cycle performance was determined by monitoring the charge–discharge run under the current density of 0.2 mA cm^{-2} and cutoff voltage range from 1.0 to 3.0 V versus Li/Li^+ at 70 °C.

3. Results and discussion

3.1. Characteristics of composite polymer electrolytes

The morphologies of the ceramic filler of nanometer-sized TiO_2 and the polymer electrolyte were characterized by

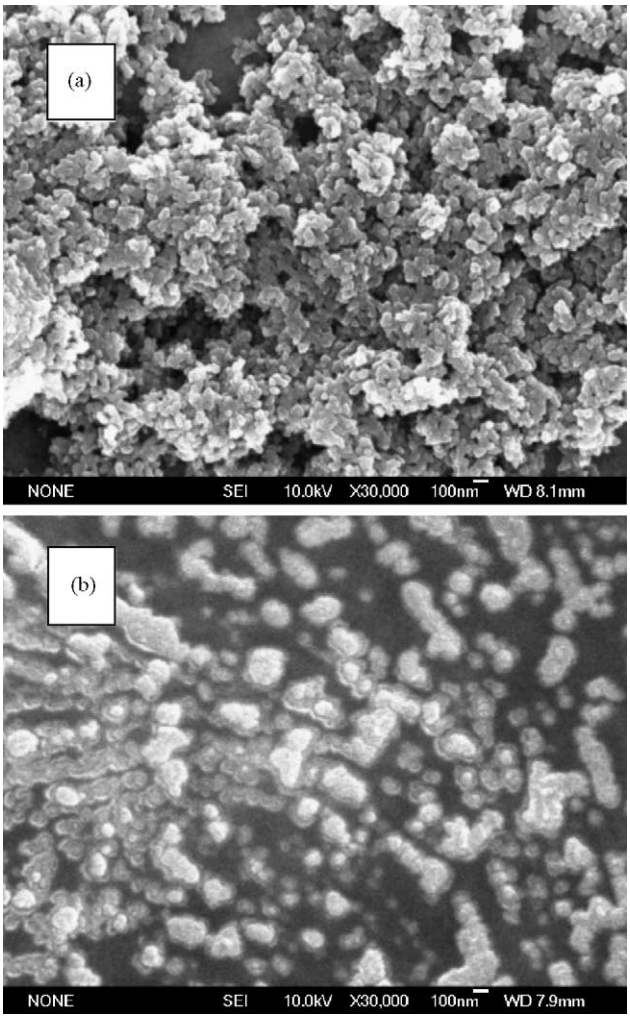

Fig. 1. SEM micrographs of (a) nanometer-TiO_2; and (b) polymer electrolyte of PEO_{20}LiTFSI + 8% TiO_2.

using a JEOL JSM-6000F-type field emission scanning electronic microscope. Fig. 1 shows the SEM images of the original TiO_2 particles and the TiO_2-added polymer electrolyte. It can be observed that TiO_2 particles distribute relatively uniformly in the polymer matrix. But due to the ultrafine nature of the original TiO_2 particles, some agglomeration occurs.

Fig. 2 shows the temperature dependence of the conductivity (from 30 to 100 °C) of the PEO_{20}LiTFSL + 8% TiO_2 and the PEO_{20}LiTFSL, respectively. The ionic conductivity of composite electrolytes with nanoparticles of TiO_2, is enhanced both below and above the crystallization temperature (about 60 °C) of PEO compared with that of ceramic-free electrolyte. In such composite electrolyte system, the nano-sized metal oxide fillers may act as "solid plasticizers" [1]. That is to say, the nano-TiO_2, due to its large surface area, kinetically inhibits recrystallization of the PEO polymer chains and promotes localized amorphous regions. However, no significant difference of XRD patterns between the TiO_2-added and ceramic-free electrolytes can

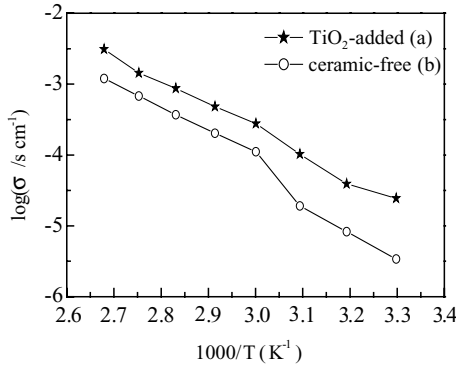

Fig. 2. Temperature dependence of the ionic conductivity of (a) PEO_{20}LiTFSI + 8% TiO_2; (b) PEO_{20}LiTFSI.

be observed, as shown in Fig. 3. So the enhancement of conductivity may be caused not only by the increase of the amount of amorphous phase in the electrolyte, but also by specific interactions between the surface groups of the ceramic particles and the lithium salt anions. The conductivity of the nanocomposite polymer electrolytes obtained reaches ca. 4.8×10^{-4} S cm^{-1} at 70 °C, which is able to satisfy the requirement of solid-state cell working at moderate temperatures.

The typical cyclic voltammogram in Fig. 4 by sweeping on a stainless steel (SS) electrode in a Li/CPE/SS cell, at a scanning rate of 5 mv s^{-1} at 70 °C, suggests that the electrolyte exhibits excellent electrochemical stability till 4 V versus Li/Li$^+$. The cathodic peak at about −0.519 V and anodic peak at about 0.293 V in the first cycle correspond to plating of lithium on the SS electrode and stripping from the SS electrode respectively, similar to the results of the reference [10]. In the following cycles, the peak locations shift a little towards the negative direction, which is caused probably by the change of the surface situation of the SS electrode. Although the lithium deposition/dissolution is not

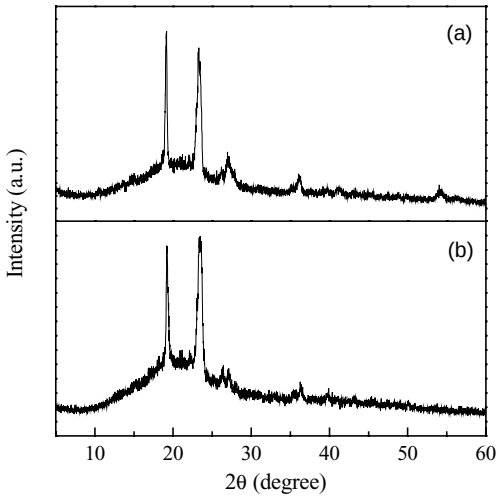

Fig. 3. XRD patterns of the CPE. (a) PEO_{20}LiTFSI + 8% TiO_2; (b) PEO_{20}LiTFSI.

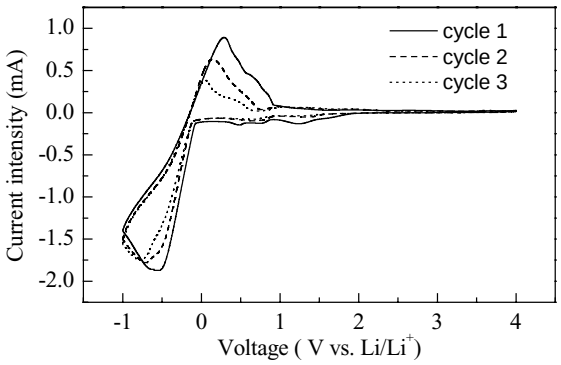

Fig. 4. Cyclic voltammetry curves of a stainless steel electrode in a cell with $PEO_{20}TFSI + 8\%\ TiO_2$ electrolyte.

completely reversible, the composite electrolyte appears to be electrochemically stable till 4 V versus Li/Li^+.

Fig. 5 shows the time evolution of the impedance spectrum in a symmetric cell, Li/CPE/Li, stored under open circuit conditions at 70 °C. The analysis of such kind of impedance spectrum has been carried out using an appropriate equivalent circuit, which denotes that the total interfacial resistance, R_i, is a combination of a generic interface resistance (R_{int}) and double-layer capacitance (Q_{dl}) [27]. The intercept of semi-circle with *x*-axis corresponds to the bulk resistance (R_b) and the value of the diameter of the semi-circle is equal to that of the whole interfacial resistance (R_i). The trends of the spectrum curves upon time evolution in Fig. 5 reveal that the interfacial resistance R_i, after an initial rise, decreases somewhat and turns to be stable for more than 30 days. This demonstrates that the passivation of lithium metal electrode is not severe but controllable in the composite polymer electrolyte. The bulk resistance (R_b) of polymer electrolyte almost keeps constant (ca. 20 Ω) over storage time, which means it does not decompose and has good dimensional stability under a certain of cell inner pressure.

3.2. Electrochemical behavior of all solid-state cells

Fig. 6 shows the typical results of cycle-life tests for the solid-state polymer electrolyte cells. When the

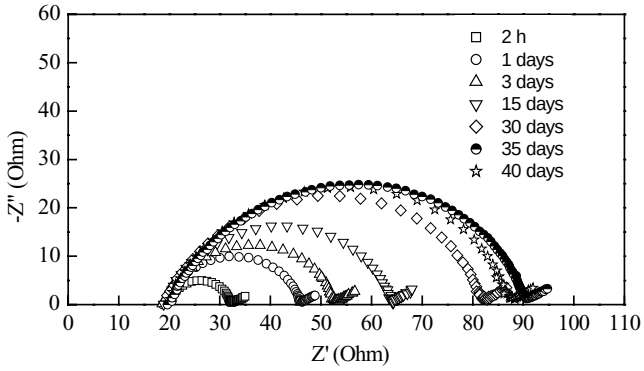

Fig. 5. Time dependence of the impedance response of Li/CPE/Li cell at 70 °C.

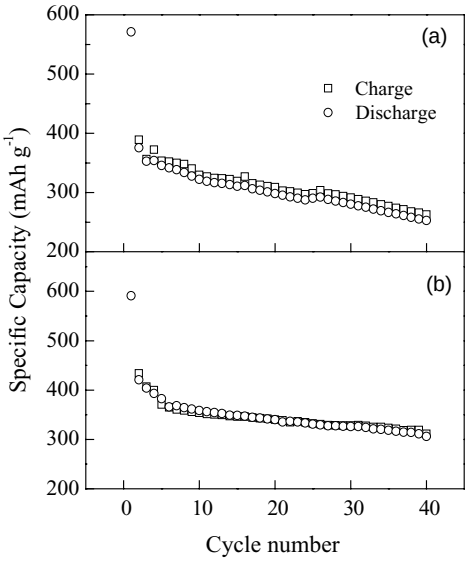

Fig. 6. Cycle characteristics of the cells with composite cathode containing. (a) PEG-free and (b) a proper amount of PEG.

composite positive electrode does not contain PEG, the charge–discharge capacities of NSC fade almost linearly as a function of cycle number in Fig. 6a. The poor penetrating ability of the electrolyte component in composite cathode and the segregation of the intercalation reaction product of lithium sulfide from electrically- and ionically-conductive phase may result in the low utilization of NSC. Low-molecular-weight PEG exhibits high ionic conductivity (magnitude order 10^{-4} S cm^{-1} at 40 °C) and low melting point (ca. 37 °C). So PEG can wet the cathode and improve the interfacial compatibility of cathode/electrolyte. Fig. 6b represents the cycleability of PEG-containing cathode. The initial discharge capacity is ca. 600 mAh g^{-1}, whereas a dramatic charge capacity drop to ca. 430 mAh g^{-1} is observed following the first discharge. The big capacity loss in the initial lithium insertion/extraction can be attributed to some irreversible conversion of the active material. The capacity fades slowly upon cycling with a charge–discharge efficiency of ca. 100% and an average capacity loss of ca. 1.5 mAh g^{-1} per cycle after the fifth cycle, remaining above 300 mAh g^{-1} after 40 cycles. The capacity fade rate of such a solid-state cell is lower than that of the gel-type polymer electrolyte cells. Due to the active component of NSC exists in the form of nano-sulfur and the improvement of contacts between different components, the cycle performance of NSC in the nanocomposite polymer electrolyte also has a great improvement compared with Li/S batteries using liquid electrolytes or solid-state polymer electrolytes [22–25].

Fig. 7 represents the typical discharge–charge profiles of the cell mentioned in Fig. 6b. In accordance with the performance showed in Fig. 6b, increased polarization of charge and discharge voltage with progressive cycling may be related to some electrochemical passivation and degradation

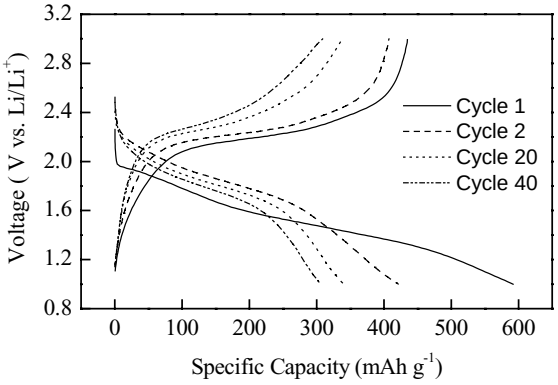

Fig. 7. Charge–discharge profiles of the all solid-state polymer electrolyte cell.

of the conductivity, which result in the capacity fade during cycling. The average charge and discharge voltage are about 2.1 and 1.9 V versus Li/Li^+. There exist two plateaus in the first discharge process, which can be further observed in the cyclic voltammogram of composite cathode at the scanning rate of $0.05\,mv\,s^{-1}$, as shown in Fig. 8. There are two cathodic peaks near 1.95 and 1.37 V, but only one anodic peak in the first cycle. From the second cycle, two almost overlapped cathodic peaks can be observed. These results, in combination with obvious difference in the cathodic and anodic peak areas at the first cycle, appear to indicate that a big kinetic difference exists for the two steps of sulfur reduction, along with some irreversible reaction during the first Li-insertion. The first reduction peak corresponds to the electrochemical reaction from sulfur to lithium polysulfide (Li_2S_n, $8 > n > 2$) and the second reduction peak is due to the change from lithium polysulfide to lithium sulfide (Li_2S or Li_2S_2). Similar results have been reported for such kind of reduction process in solid-state Li/S cells [23,25]. After the first cycle, the speed of the second step of sulfur reduction may approach to that of the first one.

In order to compare the effects of the concentration of lithium salt in electrolytes on the discharge behavior, the component of the composite cathode is kept constant as follows: 40% NSC, 15% AB, and 45% PEO_{40}(PEG) LiTFSI. Fig. 9 shows the cycling performance of Li/CPE/NSC cells with the electrolytes having different EO/Li molar ratios. The amount of the charge-carriers in the electrolytes increases with the reduction of EO/Li ratios, and so the conductivity increases in certain range of imide salt concentration and sufficient lithium ions can be supplied in time from the electrolyte during the discharge process, which results in the increase of the specific capacity. We can see from Fig. 9 that the initial discharge capacity is up to about $815\,mAh\,g^{-1}$ and remains $380\,mAh\,g^{-1}$ over 40 cycles for EO/Li = 8, which is almost as twice as that for EO/Li = 50. However, the high concentration of imide salt in PEO brings some disadvantages. The speed of capacity fade gets slightly faster due to larger volume expansion in the positive electrode under the higher insertion capacity. In addition, the polymer electrolytes become viscous and the mechanical strength decreases when dissolving more imide salt in the electrolytes, leading to some difficulty for cell assembling.

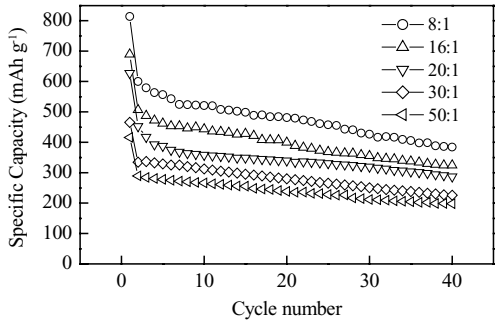

Fig. 9. Cycling performance of Li/NSC cells in different molar ratios of EO/Li.

Fig. 10 illustrates the discharge specific capacity of the cells at different operation temperatures. The cell can deliver a capacity of ca. $360\,mAh\,g^{-1}$ at the second cycle at 50 °C, yet with a large capacity loss of ca. 46% at the 40th cycle. Lower operation temperature enhances the cell resistance and thereby induces a dramatic capacity reduction, but no help for cycling stability.

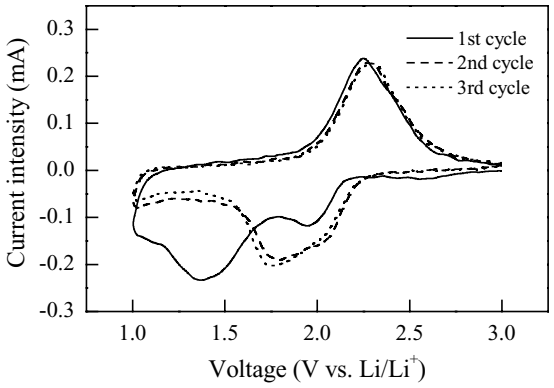

Fig. 8. Cycling voltammogram curves of composite cathode for the solid-state cell.

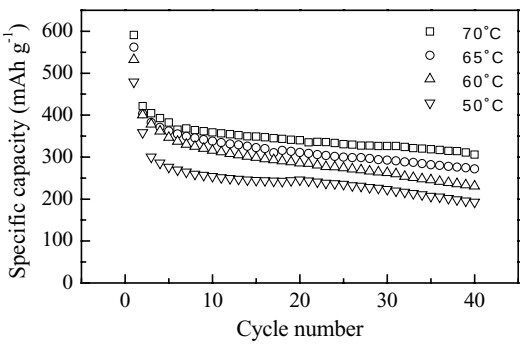

Fig. 10. Cycling performance of Li/NSC cells held at different temperatures.

4. Conclusion

All solid-state cells, constituted of metallic lithium, nanocomposite polymer electrolyte and NSC, have been assembled and electrochemically characterized. With the enhancement of lithium salt content in the electrolyte, the cycle capacity increases regularly. For a molar ratio of EO/Li = 8 in the electrolyte, the specific capacity of the cathode can reach 600 mAh g^{-1} at the second cycle, but drops to 385 mAh g^{-1} at the 40th cycle. The relatively rapid capacity loss could be, at least in part, attributed to degradation of mechanical strength of the electrolyte and instable interface property. Judging from the two sides of capacity and cyclability, the polymer electrolytes with moderate EO/Li molar ratio (such as EO/Li = 20) appear to be more suitable to match the NSC. On the other hand, addition of a small amount of PEG into the cathode increases the reversible capacity and cycle stability, which may be related to the enhanced conductivity and wettability of melt PEG. For practical application, cyclability of the composite cathode remains to be improved.

References

[1] F. Croce, G.B. Appetecchi, L. Persi, B. Scrosati, Nature 394 (1988) 456.
[2] P. Lightfood, M.A. Metha, P.G. Bruce, Science 262 (1993) 883.
[3] F.B. Dias, L. Plomp, J.B.J. Veldhuis, J. Power Sources 88 (2000) 169.
[4] J.M. Breen, H.S. Lee, X.Q. Yang, et al., J. Power Sources 89 (2000) 163.
[5] Y. Ikeda, Y. Wada, Y. Mataba, S. Murakami, S. Kohijiya, Electrochim. Acta 45 (2000) 1167.
[6] M. Watanabe, T. Hirakimoto, S. Mutoh, A. Nishimoto, Solid State Ionics 148 (2002) 399.
[7] J.-S. Chung, H.-J. Sohn, J. Power Sources 112 (2002) 671.
[8] Z. Wen, T. Itoh, M. Ikeda, N. Hirata, M. Kubo, O. Yamamoto, J. Power Sources 90 (2000) 20.
[9] J. Fan, R. Srinivasa, P.S. Fedkiw, Solid State Ionics 111 (1998) 117.
[10] J.-H. Ahn, G.X. Wang, H.K. Liu, S.X. Dou, J. Power Sources 119–121 (2003) 422.
[11] S.H. Chung, Y. Wang, L. Persi, F. Croce, S.G. Greenbaum, B. Scrosati, E. Plichta, J. Power Sources 97–98 (2001) 644.
[12] F. Croce, L. Persi, F. Ronci, B. Scrosati, Solid State Ionics 135 (2000) 47.
[13] G.B. Appetecchi, F. Croce, L. Persi, F. Ronci, B. Scrosati, Electrochim. Acta 45 (2000) 1481.
[14] B. Scrosati, F. Croce, L. Persi, J. Electrochem. Soc. 147 (2000) 1718.
[15] H.Y. Sun, H.J. Sohn, O. Yamamoto, Y. Takeda, N. Imanishi, J. Electrochem. Soc. 146 (1999) 1672.
[16] M. Watanabe, A. Nishimoto, Solid State Ionics 79 (1995) 306.
[17] Y. Xia, T. Fujieda, K. Tatsumi, P.P. Prosini, T. Sakai, J. Power Sources 92 (2001) 234.
[18] P. Villano, M. Carewska, G.B. Appetecchi, S. Passerini, J. Electrochem. Soc. 149 (2002) A1282.
[19] L. Persi, F. Croce, B. Scrosati, E. Plichta, M.A. Hendrickson, J. Electrochem. Soc. 149 (2002) A212.
[20] E. Levi, E. Zinigrad, H. Teller, M.D. Levi, D. Aurbach, J. Electrochem. Soc. 145 (1998) 3440.
[21] H. Yamin, A. Gorenshtein, J. Penciner, Y. Sternberg, E. Pled, J. Electrochem. Soc. 135 (1988) 1045.
[22] D. Marmorstein, T.H. Yu, K.A. Striebel, F.R. Mclarnon, J. Hou, E.J. Cairns, J. Power Sources 89 (2000) 219.
[23] J. Shim, K.A. Striebel, E.J. Cairns, J. Electrochem. Soc. 149 (2002) A1321.
[24] E. Peld, T. Sternberg, A. Gorenshtein, Y. Lavi, J. Electrochem. Soc. 136 (1989) 1621.
[25] B.H. Jeon, J.H. Yeon, K.M. Kim, I.J. Chung, J. Power Sources 109 (2002) 89.
[26] J.L. Wang, J. Yang, J.Y. Xie, N.X. Xu, Adv. Mater. 14 (2002) 963.
[27] G.B. Appetecchi, S. Passerini, J. Electrochem. Soc. 149 (2002) A891.